Synthesis of Asymmetric Flat-Top Birefringent Interleaver Based on Digital Filter Design and Genetic Algorithm

P. J. Pinzón, C. Vázquez, I. Pérez, and J. M. Sánchez Pena

Grupo de Displays y Aplicaciones Fotónicas, Departamento de Tecnología Electrónica, Universidad Carlos III de Madrid, 28911 Leganés, España

Abstract: A flexible and fast synthesis method for designing asymmetric interleavers with flat-top, low dispersion, adjustable isolation, and bandwidths at both outputs is proposed. Interleavers are designed on birefringent technology allowing linear-phase designs. *Z*-transform properties and digital filter design techniques are used for designing interleavers under a set of specifications. At a second level, a genetic algorithm optimization approach allows improving the interleaver design adjusting the minimum isolation, at both outputs, below −43 dB and the stop bandwidths to specific normalized values of ±0.15 and ±0.3, with zero dispersion at one output. Improvement of the interleaver order and dispersion below ±50 ps/nm at both outputs are also reported.

Index Terms: Interleavers, birefringent plates, genetic algorithms (GA), finite impulse response (FIR) filters, fiber optic systems.

1. Introduction

Optical interleavers are filters that separate an incoming spectrum into two complementary set of periodic spectra (odd and even channels) or combine them into a composite spectrum. They play a key role in dense wavelength division multiplexing (DWDM) systems, as in gain equalization, dispersion compensation, prefiltering, and channels add/drop applications.

Asymmetric interleavers separate the odd and even channels with different pass bandwidths. In fact, symmetric interleavers are a particular case in which both channel groups have the same pass bandwidths. As an example, asymmetric interleavers allow accommodating the next-generation systems with 40-Gb/s signals in the larger bandwidth and maintaining legacy systems with 10-Gb/s signals in the smaller bandwidth [1], [2]. This is an effective and low-cost solution to extend the existing legacy network capacity, for systems upgrade and bidirectional network implementations.

Many approaches have been demonstrated to implement interleavers, based on interference effects due to their intrinsic periodic response. Most interleavers are based on Michelson interferometers, Mach–Zehnder interferometer (MZI) or birefringent filter (BF) principles, and they are implemented in bulk optics, all-fiber, or integrated optics technologies [3], [4]. In these configurations, different phase-dispersion elements, such as ring resonators (RRs), Gires–Tournoise etalons, and resonant cavities, may be used to improve their boxlike characteristic [5], [6]. But those solutions increase considerably the interleaver's chromatic dispersion (CD) and its sensitivity to

manufacturing tolerances. Interleavers can also be implemented by using Fabry–Perot filters [7], Bragg diffraction gratings, and arrayed waveguide gratings (AWG) [4].

Birefringent interleavers are implemented in bulk optics and use lattice structures to get flat-top designs. These interleavers are highly reliable and easy to manufacture, use passive temperature compensation schemes, and require polarization diversity to avoid polarization-dependent loss (PDL) [8]. Since they operate in transmission, their transfer functions in the Z-domain have only zeros and can be designed to have zero dispersion without compensation. CD is a critical factor in 40-Gb/s systems and beyond. Interleavers with large CD use compensation schemes, based on double-pass designs with opposite CD slops, to cancel the overall CD or use novel configuration mixing MZI and Gires–Tournoise etalons [9]. These additional elements increase the insertion loss and device complexity, but even manufacturing tolerances still cause a small amount of CD [8]. This is the reason for being flat-top birefringent interleavers an attractive choice in high data rate applications [10].

In general, lattice interleaver designs include methods based on Fourier series, digital filter design, and computational optimization, but most of them do not take into account a simultaneous analysis of both outputs, which is an essential aspect in interleavers design. Fourier-series-based method uses a lattice structure with delay lines multiples of a unit value [4]. This method uses M-simultaneous equations to determine an M-order filter structure to fit an ideal transfer function shape. It requires high-order filters to obtain low side lobes.

Digital filter design method is based on the mathematical equivalence of the finite impulse response (FIR) filters and the lattice interleavers with delay lines of a constant value [1], [10], [11]. This method uses a FIR filter with transfer function $H(z)$, to find the structural parameters of the equivalent lattice interleaver in an iterative way. Any FIR filter synthesis method can be used to get $H(z)$; this allows good control over the design parameters. But previous developments of this design method applied to interleaver designs, as those reported in [10], do not consider the reciprocal output (e.g., even channels); neither CD is considered, limiting the control over fundamental parameters at both interleaver's outputs.

Computational-optimization-based methods use a global optimization algorithm, such as genetic algorithm (GA), to fit a specific transfer function to an ideal response, by finding the best variable values. In the synthesis of interleavers, by only using this method, the parameters at both outputs can be controlled but with low precision and for a fixed interleaver order [12].

In this paper, a synthesis method of asymmetric flat-top birefringent interleavers is proposed. It conjugates the advantages of digital filter design methods, in the Z-transform domain, and computational optimization. It allows accurate design at both outputs (odd and even channels) in terms of key parameters such as bandwidths, isolation, ripple, CD, and asymmetry. GA allows parameter optimization at both outputs with the required behavior in a simple and effective way. The proposed method allows also designing interleavers with minimum dispersion and order.

This paper is organized as follows. Section 2 is devoted to synthesis method of lattice birefringent interleavers in the Z-transform domain for designing an asymmetric interleaver. Section 3 describes the GA optimization process applied to a digital filter design through two optimization examples, one based on dispersion and the other on bandwidths and isolation. Finally, the proposed synthesis process is discussed on Section 4, and conclusions are given on Section 5.

2. Birefringent Interleaver Filter

A flat-top BF has a lattice structure consisting on a stack of M birefringent plates, with different azimuth angles α_n, with $n = 1, 2, \ldots, M$, relative to xy-plane, bounded between linear polarizers (LPs). LP at the output is called analyzer and has an azimuth angle α_{M+1}. Filter operation is based on the interference of an input light beam with multiple delayed versions of itself [13], [14]. Fig. 1 shows the schematic of a flat-top BF. In this scheme, phase shifters can be used to alter the polarization of the light beams between consecutive birefringent plates.

Each birefringent plate produces an unitary delay Γ, which is a function of the input beam with frequency f and speed c, and the birefringent medium of thickness d and birefringence Δn. This
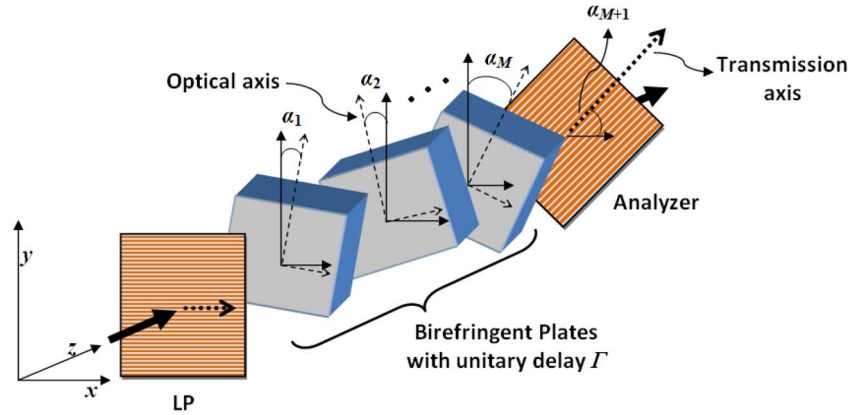
Fig. 1. Lattice structure of a BF.

delay is expressed as:

$$\Gamma = \frac{2\pi}{c} f \Delta n d. \tag{1}$$

The contribution of multiplying M birefringent plates is represented by the characteristic matrix Q^M, which is expressed as:

$$Q^M = \prod_{n=1}^{M} [R(\alpha_n)] \times [W(\Gamma)] \times [R^{-1}(\alpha_n)] \tag{2}$$

where n is the stage number, R is a rotation matrix respect to the xy-plane, and W is the Jones matrix of the birefringent plate. These matrices are given by:

$$R(\alpha_n) = \begin{pmatrix} \cos(\alpha_n) & \sin(\alpha_n) \\ -\sin(\alpha_n) & \cos(\alpha_n) \end{pmatrix}, W(\Gamma) = \begin{pmatrix} e^{\frac{-i\Gamma}{2}} & 0 \\ 0 & e^{\frac{i\Gamma}{2}} \end{pmatrix}. \tag{3}$$

Considering that the analyzer has an azimuth angle, α_{M+1}, the output relative to the xy-plane is given by:

$$[Q^{M+1}] = [Q^M] \times [R(\alpha_{M+1})] \times [P_X] \times [R^{-1}(\alpha_{M+1})] \tag{4}$$

where P_X is the Jones matrix of a LP parallel to the x-axis, and it is given by:

$$P_X = \begin{pmatrix} 1 & 0 \\ 0 & 0 \end{pmatrix}. \tag{5}$$

$[Q^{M+1}]_{11}$ and $[Q^{M+1}]_{21}$ represent the output polarization components parallel to the x-axis (x-polarized), i.e., Tx, and parallel to the y-axis (y-polarized), i.e., Ty, called also bar and cross outputs, respectively, when the input beam is x-polarized.

For interleaving applications, the bar and cross outputs are separated by using a polarization beam splitter element.

2.1. Transfer Function and Z-Transform

By analogy with an ordinary MZI, the two optical axis of the birefringent medium can be regarded as M pairs of delay lines, as part of the interfering arms. And the azimuth angles, in the form of relative azimuth angles θ_{n-1} ($\theta_0 = \alpha_1, \theta_1 = \alpha_2 - \alpha_1, \ldots, \theta_{M-1} = \alpha_M - \alpha_{M-1}, \theta_M = \alpha_{M+1} - \alpha_M$, see Fig. 1), are analog to $M + 1$ coupling constants. Then, Jinguji and Kawachi synthesis method [15] can be used for synthesizing flat-top BFs, as already reported [1] and [10]. In this paper, the relation

between BFs and the *Z*-transform domain is analyzed following a similar procedure to that presented in [16]. It is considered that there are no phase shifters and there is no loss in any of the elements, so that their transfer functions are unitary. The dispersion of the elements is neither considered.

The unitary delay Γ can be related to the *Z*-transform domain, with $z = exp(i\Gamma)$. Then, from (3), $W(z)$ can be expressed as:

$$W(z) = \begin{pmatrix} z^{-\frac{1}{2}} & 0 \\ 0 & z^{\frac{1}{2}} \end{pmatrix}. \tag{6}$$

From (2), the characteristic matrix $Q^M(z)$ is a 2×2 unitary matrix, which can be expressed as follows:

$$Q^M(z) = \begin{bmatrix} H^M(z) & -F^M(z)^* \\ F^M(z) & H^M(z)^* \end{bmatrix} \tag{7}$$

where superscript * denotes the Hermitian conjugation (reverse polynomial).

The terms $H^M(z)$ and $F^M(z)$ are polynomials of degree M, where $H^M(z)$ is the bar-transfer function and $F^M(z)$ is the cross-transfer function. If the input beam is *x*-polarized, they can be expressed as:

$$H^M(z) = \left(\sum_{k=0}^{M} a_k z^{-k} \right) z^{M/2} \tag{8}$$

$$F^M(z) = \left(\sum_{k=0}^{M} b_k z^{-k} \right) z^{M/2} \tag{9}$$

where coefficients a_k and b_k are the impulse response of the FIR filters of order M, $H^M(z)$ and $F^M(z)$, respectively.

From (7), it is shown that Q^M is an unimodular matrix, so their components are related by:

$$H^M(z)H^M(z)^* + F^M(z)F^M(z)^* = 1. \tag{10}$$

Therefore, knowing one of the two transfer functions in *Z*, the other is immediately defined.

The following recursive identity is used to relate $H^M(z)$ and $F^M(z)$ with the structural parameters of the equivalent birefringent interleaver [16]:

$$[Q_M][Q^{M-1}] = [Q^M] \tag{11}$$

where superscript $M-1$ indicates that the matrix is the result of multiplying the $M-1$ first delay stages, resulting in $M-1$ order filters, and subscript M indicates that it is the transfer matrix of the *M*th stage. Multiplying both sides of (11) by the inverse of Q_M, the following matrix relationship is obtained:

$$\begin{bmatrix} H^{M-1}(z) \\ F^{M-1}(z) \end{bmatrix} = \begin{bmatrix} \cos(\theta_M)z^{1/2} & -\sin(\theta_M)z^{1/2} \\ \sin(\theta_M)z^{-1/2} & \cos(\theta_M)z^{-1/2} \end{bmatrix} \begin{bmatrix} H^M(z) \\ F^M(z) \end{bmatrix}. \tag{12}$$

Then, from (12), $H^{M-1}(z)$ and $F^{M-1}(z)$ can be written as:

$$H^{M-1}(z) = \left\{ \sum_{k=1}^{M} [a_k\cos(\theta_M) - b_k\sin(\theta_M)]z^{-k} \right\} z^{(M+1)/2} + [a_0\cos(\theta_M) - b_0\sin(\theta_M)]z^{(M+1)/2} \tag{13}$$

$$F^{M-1}(z) = \left\{ \sum_{k=0}^{M-1} [a_k\sin(\theta_M) + b_k\cos(\theta_M)]z^{-k} \right\} z^{(M-1)/2} + [a_M\sin(\theta_M) + b_M\cos(\theta_M)]z^{-(M+1)/2}. \tag{14}$$

Both polynomials are obtained by multiplying $M-1$ matrices. Comparison of previous equations to (8) and (9) reveals that the terms outside the summation in (13) and (14) should be zero, so that
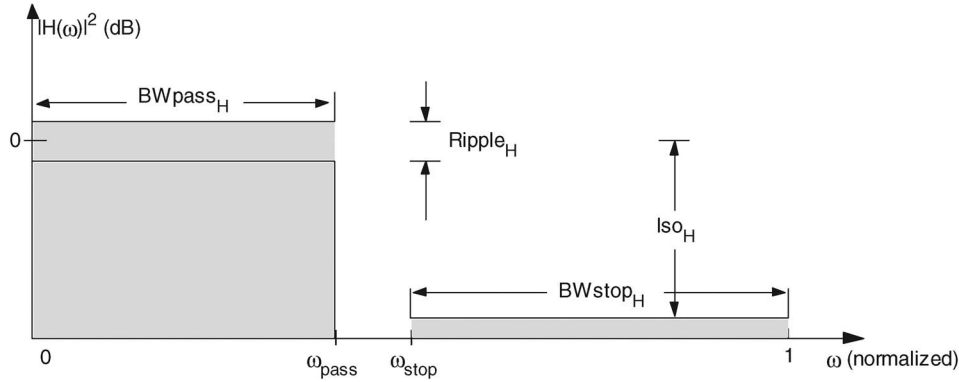
Fig. 2. Filter specifications and parameters.

the value of the Mth relative azimuth angle θ_M is given by:

$$\tan(\theta_M) = \frac{\sin(\theta_M)}{\cos(\theta_M)} = \frac{a_0}{b_0} = -\frac{b_M}{a_M}. \tag{15}$$

Knowing θ_M, the previous coefficient groups a_k^{M-1} and b_k^{M-1}, with $k = 0, 1, \ldots, M - 1$, can be obtained, which represent the coefficients of the $M - 1$ order filters obtained by multiplying the $M - 1$ previous stages. The whole recursive process is done using the next three equations:

$$a_k^{n-1} = a_{k+1}^n \cos(\theta_n) - b_{k+1}^n \sin(\theta_n) \tag{16}$$

$$b_k^{n-1} = a_k^n \sin(\theta_n) + b_k^n \cos(\theta_n) \tag{17}$$

$$\tan(\theta_{n-1}) = \frac{a_0^{n-1}}{b_0^{n-1}} = -\frac{b_{n-1}^{n-1}}{a_{n-1}^{n-1}} \tag{18}$$

where n is replaced in inverse order $n = M, M - 1, \ldots, 1$. For each n value, using (16) and (17), the coefficient groups a_k^{n-1} and b_k^{n-1}, with $k = 0, 1, \ldots, n - 1$, are obtained. Then, (18) is used to get θ_{n-1} and again starts the recursive process.

Finally, the azimuth angle of the nth birefringent plate is $\alpha_n = \sum_{m=0}^{n-1} \theta_m$, and the azimuth angle of the analyzer is $\alpha_{M+1} = \sum_{m=0}^{M} \theta_m$.

For simplicity, from now on, $H^M(z)$ and $F^M(z)$ will be referred as $H(z)$ and $F(z)$, respectively.

2.2. Birefringent Interleaver Design Example

In this section, a simple process to design two reciprocal FIR filters is described, as well as the method to find their equivalent birefringent interleaver.

There are many algorithms and functions to design FIR filters. In this paper, Parks–McClellan optimal equiripple FIR filter design algorithm is implemented by using MATLAB functions [17]. Main parameters considered in the low-pass filter design (see Fig. 2) are the normalized lower (ω_{pass}) and higher (ω_{stop}) cut frequencies, the ripple in the pass band ($Ripple_H$), and the isolation in the stop band (Iso_H). Other related parameters are the normalized pass bandwidth $BWpass_H$ and stop bandwidth $BWstop_H$.

All previous parameters are defined for $H(z)$. In the same way, the ripple in the pass band of $F(z)$, the isolation in its stop band, its pass bandwidth, and its stop bandwidth are defined by $Ripple_F$, Iso_F, $BWpass_F$, and $BWstop_F$, respectively.

The order, stop bandwidth, ripple, and isolation of only one output can be well designed using previous reported methods [1], [10]. Specifications of both outputs can be controlled by relating the

TABLE 1

Specifications of the interleaver design example

Parameter	$H(z)$		$F(z)$	
	Symbol	Value	Symbol	Value
25dB Stop-Bandwidth	$BWstop_H$	±0.15	$BWstop_F$	±0.30
Pass-Band Ripple (dB)	$Ripple_H$	≤1.37×10⁻³ over 30% FSR	$Ripple_F$	≤1.37×10⁻³ over 15% FSR
Stop-Band Isolation (dB)	Iso_H	≤-25 over 15% FSR	Iso_F	≤-25 over 30% FSR
Filter Order	M	≤10	M	≤10

TABLE 2

Coefficients of the filter $H(z)$, a_k, and $F(z)$, b_k. Relative angles, θ_{n-1}, and azimuth angles, α_n, of the equivalent birefringent interleaver

k	a_k	b_k	n	θ_{n-1}	α_n
0	0.0197	0.2378	1	-1.4884	-1.4884
1	-0.0587	-0.4784	2	-0.0798	-1.5682
2	0.0043	0.3545	3	-0.2583	-1.8265
3	0.5347	-0.0169	4	1.0378	-0.7887
4	0.5347	-0.0956	5	1.0380	0.2494
5	0.0043	0.0001	6	-0.2582	-0.0088
6	-0.0587	0.0064	7	-0.0801	-0.0890
7	0.0197	-0.0016	8	0.0824	-0.0066

ripple of one output with the isolation of the other output. From (10), $|F(\omega)|^2 = 1 - |H(\omega)|^2$, then $Ripple_H$ can be related to Iso_F by the following expression:

$$Ripple_H(dB) = 10\log_{10}\left[10^{\frac{Iso_F(dB)}{10}} + 1\right]. \qquad (19)$$

A design example of an asymmetric BF is described below to show the potential of the proposed method. Interleaver specifications are shown in Table 1, where FSR is the free spectral range; these values were extracted from those reported in [18].

ω_{pass}, ω_{stop}, and Iso_F are set to 0.15, 0.30, and -30 dB, respectively, then from (19), $Ripple_H$ is set to 4.34×10^{-3} dB, to satisfy the interleaver's requirements of Table 1. The resulting filter $H(z)$ is a seventh-order filter, and its coefficients a_k are shown in Table 2.

Now, reciprocal filter $F(z)$ is inferred using (10). This equation allows getting the $2M$ zeros of $F(z)F(z)^*$, which appear as pair of $(b_k, 1/b_k^*)$, with $k = 0, \ldots, M$. Using spectral factorization, one of each pair $(b_k, 1/b_k^*)$ must be selected for $F(z)$ or $F(z)^*$. We chose the M zeros inside the unit circle to infer $F(z)$. The resulting normalized coefficients b_k are shown in Table 2.

Knowing $H(z)$ and $F(z)$, (16)–(18) are used to find the relative azimuth angles θ_{n-1}, which define the azimuth angles α_n of the seven birefringent plates ($M = 7$) plus the analyzer. These angles are also shown in Table 2.

Normalized dispersion is defined as the derivate of the group delay [19] with respect to the normalized frequency, ω_n, and it is calculated using the following expression:

$$D_n = 2\pi \frac{d}{d\omega_n}\left(-\frac{d}{d\omega_n}\Theta(\omega_n)\right) \qquad (20)$$

where Θ is the phase or argument of the filter response. Then, the filter dispersion in absolute units (in s/m) is given by:

$$D = -c\left(\frac{T}{\lambda}\right)^2 D_n \qquad (21)$$

where T is the filter period ($T = 1/FSR$), and c is the speed of the light.
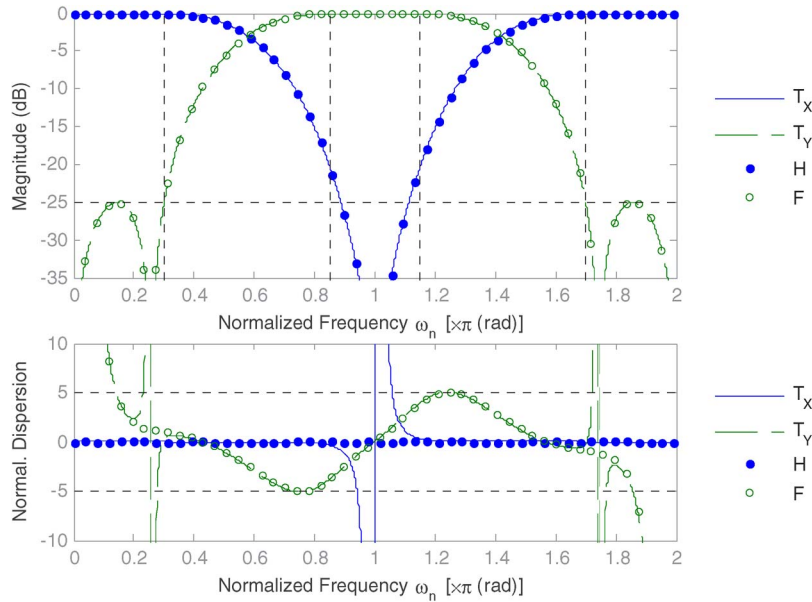
Fig. 3. Birefringent interleaver design results.

TABLE 3

Analysis results of the asymmetric birefringent interleaver design. $M = 7$

Parameter	T_x		T_y	
	Normalized FSR = 2	with FSR = 100GHz at 1550nm	Normalized FSR = 2	with FSR = 100GHz at 1550nm
0.5dB Pass-Bandwidth	±0.4316	43.16 GHz	±0.2715	27.15 GHz
3.0dB Pass-Bandwidth	±0.5781	57.81 GHz	±0.4219	42.19 GHz
25dB Stop-Bandwidth	±0.1133	11.33 GHz	±0.3080	30.80 GHz
Pass- Band Ripple (dB)	13.53×10^{-3} over 30% FSR		40.02×10^{-3} over 15% FSR	
Stop-Band Isolation (dB)	≤-20 over 15% FSR ≤-25 over 11% FSR		-25 over 31% FSR	
Max CD at 3.0dB Pass-Band	0	0 ps/nm	±5.05	±63 ps/nm

Fig. 3 shows the magnitude response and normalized dispersion of $H(z)$ and $F(z)$, and the resulting interleaver with outputs Tx and Ty. In this figure, the equivalence between the magnitude response and the dispersion of the digital filters and the optical interleaver are observed.

Table 3 shows the performance of the interleaver shown in Fig. 3. The resulting 0.5-dB normalized pass bandwidth of Tx and Ty are ± 0.4316 and ± 0.2715, respectively. In an interleaver with FSR of 100 GHz, those normalized values represent bandwidths of 43.16 GHz and 27.15 GHz. Since $H(z)$ is designed to be linear-phase filter, Tx has zero dispersion (CD) in the pass band. This characteristic of Tx is ideal for applications in 40-Gb/s systems. On the other hand, the normalized dispersion of Ty is ± 5.05; this is equal to a dispersion, in absolute units, of ± 63 ps/nm in an interleaver with $FSR = 100$ GHz operating at a wavelength of 1550 nm. This value is comparable with the dispersion reported on [18] but can be further improved as it is described in the discussion section. In Table 2, it is shown that the 25-dB normalized stop bandwidth of Tx and Ty have relative errors of 24.47% and 2.67% from the expected values of ± 0.15 and ± 0.30, respectively (see also Table 1).

In the next section, an optimization process is proposed to reduce the error between the designed interleaver parameters and the expected design parameters, including the dispersion of the output Ty.

3. GA for Interleaver Design Optimization

The synthesis method that is proposed uses digital filter design algorithms for interleavers' optimization, which can be regarded as black-box functions. Therefore, the optimization problems must be solved using a global optimization algorithm [20].

The GA is a global optimization algorithm that, due to its random nature, improves the possibilities of finding a global solution. GA solves optimization problems by mimicking the principles of biological evolution [20]. GA minimizes an objective function $Fobj(\boldsymbol{x})$, where $\boldsymbol{x}$ is a vector of variables, considering these variables as chromosomes, $\boldsymbol{x}$ as an individual, and the group of individuals as a population. This approach has been previously used in designing photonic-crystal waveguide interleavers [21] and birefringent interleavers [1], [12], but not in combination with a digital signal processing approach.

GA can be used to optimize $H(z)$, adjusting T_x and T_y to the expected response (see Tables 1 and 2). Using GA in combination with FIR filter design algorithms gives simplicity, since the only required variables to define the vector $\boldsymbol{x}$ are the normalized lower (ω_{pass}) and higher (ω_{stop}) cut frequencies, and the interleaver's isolation Iso, then the vector of variables $\boldsymbol{x}$ is given by:

$$\boldsymbol{x} = [\omega_{pass}, \quad \omega_{stop}, \quad Iso]. \tag{22}$$

It is efficient, because the procedure is fast (few seconds) and slightly independent of the interleaver's order. And it is flexible, since it allows adjusting specific parameters.

Next, two optimization examples are shown to illustrate the proposed procedure.

3.1. Optimizing Bandwidth and Isolation

It is defined the next objective function for adjusting the bandwidth and isolation of $|H(\omega)|^2$ and $|F(\omega)|^2$ to the desired values:

$$F_{obj1}(\boldsymbol{x}) = \left(\left| \frac{0.15 - Bw_{stop}H}{0.15} \right| + \left| \frac{0.30 - Bw_{stop}F}{0.30} \right| + \left| \frac{Iso_H - Iso_F}{Iso_H} \right| \right) \times 100. \tag{23}$$

All terms of (23) depend on $\boldsymbol{x}$. The first two terms adjust the bandwidths to the specific values of ± 0.15 and ± 0.3, and the third term ensures that the isolation of both outputs is equal. Stop bandwidths are measured at -25 dB, then the minimum isolation at the stop band will be always less that -25 dB.

Optimization is performed by setting the searching bounds from $\boldsymbol{x} = [0.05 \; 0.55 \; 25]$ to $\boldsymbol{x} = [0.45 \; 0.95 \; 60]$. In this optimization, the error of $Fobj_1(\boldsymbol{x})$ is 0.1144%, with the following combination of variables $\boldsymbol{x}_1 = [0.2242 \; 0.0998 \; 43.3646]$. The minimum value of an objective function depends on the considered parameters; in the case of $Fobj_1(\boldsymbol{x})$, its minimum value is zero.

Fig. 4 shows the comparison between the interleaver designed in the previous section with output Tx and Ty and the optimized interleaver of this example with outputs Tx_1 and Ty_1. This optimization adjusts the isolation of Tx_1 and Ty_1 to -43.28 dB and their stop bandwidths to the expected values of ± 0.15 and ± 0.30, respectively. This optimization also increases the normalized dispersion of Ty_1 from ± 5.05 to ± 6.8, which corresponds to ± 85 ps/nm in an interleaver with $FSR = 100$ GHz operating at 1550 nm. The dispersion increment is the cost of improving the filter response, and it is mainly due to the fact that the optimized filter has an order $M = 9$ that it is higher than the order of the previous filter $M = 7$. Anyhow, in previous designs [10], it is reported an isolation of -40 dB for only one output and using an order $M = 14$, so it has a higher dispersion.

Table 4 shows the normalized parameters of the optimized interleaver shown in Fig. 4, and the respective absolute values for an interleaver with unitary delay Γ, designed to have a $FSR = 100$ GHz (50-GHz channel spacing) operating at 1550 nm. In [3], the design of Γ to fulfill these conditions with an athermal configuration can be found, showing the manufacturing feasibility of the proposed design.
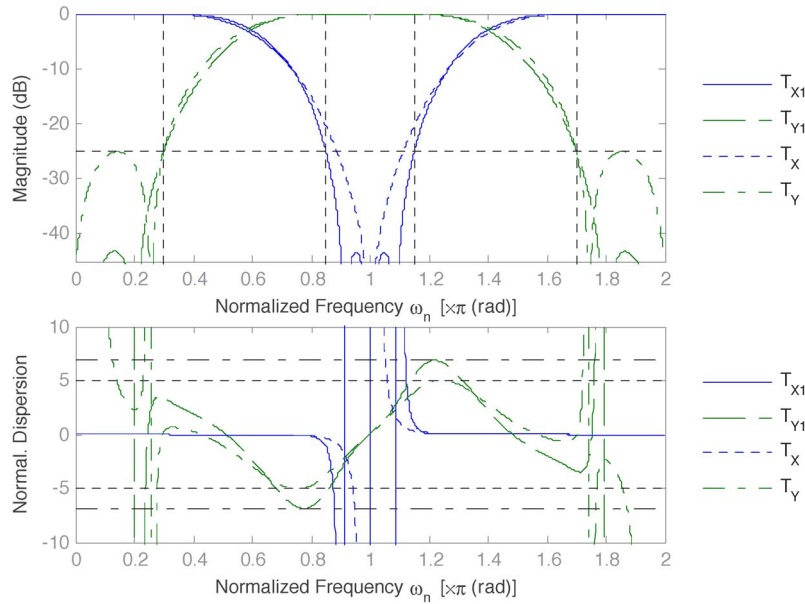
Fig. 4. Magnitude response and normalized dispersion of the Birefringent Interleaver with outputs Tx and Ty and the interleaver optimized using GA with outputs $Tx1$ and $Ty1$.

TABLE 4

Analysis results of bandwidth and isolation optimization (first optimization). Resulting interleaver's order $M = 9$

Parameter	T_{x1}		T_{y1}	
	Normalized FSR = 2	with FSR = 100GHz at 1550nm	Normalized FSR = 2	with FSR = 100GHz at 1550nm
0.5dB Pass-Bandwidth	±0.4568	45.68 GHz	±0.2703	27.03 GHz
3.0dB Pass-Bandwidth	±0.5986	59.86 GHz	±0.4013	40.13 GHz
25dB Stop-Bandwidth	±0.1501	15.01 GHz	±0.3000	30.00 GHz
Pass- Band Ripple (dB)	13.68×10^{-3} over 30% FSR		13.80×10^{-3}	
Stop-Band Isolation (dB)	≤-25 over 15% FSR		≤-25 over 30% FSR	
	-43.28 over 10% FSR		-43.28 dB at 22% FSR	
Max CD at 3.0dB Pass-Band	0	0 ps/nm	±6.86	±85.66 ps/nm

3.2. Optimizing BW Considering Dispersion

The pass bandwidths can be further optimized, without significantly increasing the dispersion, by using the following objective function:

$$F_{obj2}(x) = \left| \frac{0.15 - Bw_{stop}H}{0.15} \right| \times 100 + \left| \frac{0.30 - Bw_{stop}F}{0.30} \right| \times 100 + D_{n\_maxF} + c_1 M. \quad (24)$$

First and second terms of $Fobj_2(x)$ adjust the bandwidths to the specific values of ±0.15 and ±0.3; the third term minimizes the maximum normalized dispersion of $F(z)$, i.e., D_{n_maxF}, and the last term minimizes the interleaver's order, which also reduces D_{n_maxF}. In this objective function, it is not included the isolation because it is not possible to optimize simultaneously all variables in an effective way. Anyway, as stated in previous example, stop bandwidth is measured at -25 dB, then isolation value will always be less that -25 dB. In this function, the weighting coefficient $c_1 = 2$ is used to give relative importance rank to the interleaver's order M.
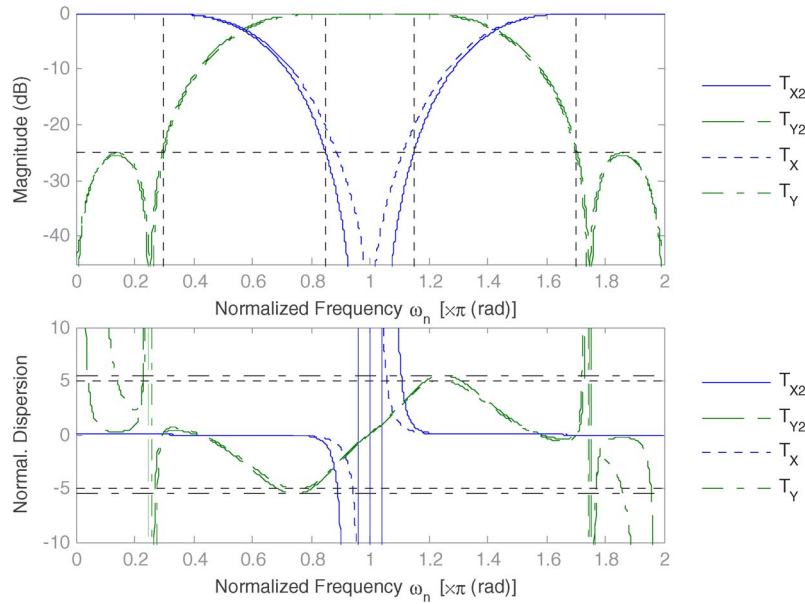
Fig. 5. Magnitude response and normalized dispersion of the Birefringent Interleaver with outputs *Tx* and *Ty* and the Interleaver optimized using GA with outputs *Tx*2 and *Ty*2.

TABLE 5

Analysis results of bandwidths optimization considering dispersion (second optimization). Resulting interleaver's order M = 7

Parameter	T_{x2}		T_{y2}	
	Normalized FSR = 2	with FSR = 100GHz at 1550nm	Normalized FSR = 2	with FSR = 100GHz at 1550nm
0.5dB Pass-Bandwidth	±0.4235	42.35 GHz	±0.2900	29.00 GHz
3.0dB Pass-Bandwidth	±0.5671	56.71 GHz	±0.4329	43.29 GHz
25dB Stop-Bandwidth	±0.1499	14.99 GHz	±0.2942	29.42 GHz
Pass- Band Ripple (dB)	18.17×10^{-3} over 30% FSR		14.00×10^{-3} over 15% FSR	
Stop-Band Isolation (dB)	≤-25 over 15% FSR		-25dB over 30% FSR	
Max CD at 3.0dB Pass-Band	0	0 ps/nm	±5.52	±68.93 ps/nm

Optimization is performed by setting the same searching bounds than in previous example. The resulting error of $F_{obj2}(\boldsymbol{x}) = 21.52\%$, with a combination of variables $\boldsymbol{x}_2 = [0.2921\ 0.1689\ 28.9235]$. The order of $H(z)$ will be $M \geq 3$, due to the implemented function [17]; therefore, the theoretical minimum value of $F_{obj2}(\boldsymbol{x})$ is 6, and it increases with M.

Fig. 5 shows a comparison between the interleaver designed in Section 2.2, with outputs *Tx* and *Ty*, and the optimized interleaver of this section with outputs *Tx*2 and *Ty*2. This optimization example adjusts the stop bandwidths of $H(z)$ and $F(z)$ to the expected values of ±0.15 and ±0.30, respectively, and improves the isolation of *Tx* below −25 dB over 15% FSR, with a minimum increment of D_{n_maxF}, from ±5.05 to ±5.52, maintaining the interleaver's order in $M = 7$. The isolation of *Ty* is also improved below −25 dB over 30% FSR. The minimum isolations at the stop bands of $H(z)$ and $F(z)$ are not exactly equal, since this parameter is not included in $Fobj_2(x)$.

Table 5 shows the normalized parameters of the optimized interleaver shown in Fig. 5. These results show that this optimization example adjusts the pass bandwidths to the desired values and improves the isolation of Ty_2 with slight variations in dispersion, in comparison with the nonoptimized interleaver (see Table 3).
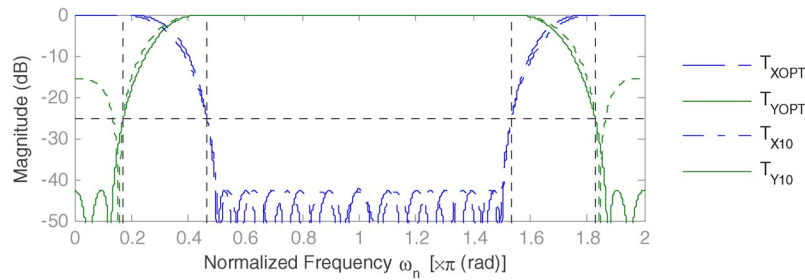
Fig. 6. Direct, Tx_{10}, and crossed, Ty_{10}, outputs of the BF designed in [10], $M = 14$. Direct, Tx_{OPT}, and crossed, Ty_{OPT}, outputs of an optimized interleaver, $M = 20$.

4. Discussion

Although synthesis of flat-top BFs based on digital filter design methods have been previously reported, they have just considered only the design of one of the outputs [10]. But interleavers' performance is based on odd and even channels spatial separation, so both outputs must be considered. As an illustrative example, the direct (Tx_{10}) and crossed (Ty_{10}) outputs of the BF designed in [10] are shown in Fig. 6.

It is shown that Tx_{10} output isolation is -43 dB, being a good value for a single output filter. However, Ty_{10} output isolation is only -15.5 dB. This isolation value is low for being used as an interleaver. A new optimized design is shown at Fig. 6, with outputs Tx_{OPT} and Ty_{OPT}, with -42 dB isolation at both outputs, maintaining the pass-band and stop-band characteristics of Tx_{10}.

Add–drop filter designs based on infinite impulse response filters [22] are neither applicable to asymmetric interleaver applications, as they are symmetric and have intrinsically higher dispersion. The design method proposed in Section 2 is simple, fast, and effective. This method, relaying on digital filter design algorithms, allows designing the stop bandwidth and isolation of each interleaver outputs independently. This is a fundamental property in birefringent asymmetric interleaver synthesis. Further adjustments of specific parameters can be carried out in a second step by using GAs as described in Section 3.

The results of Figs. 3–5 show that it is possible to design birefringent interleavers with an output with zero dispersion. For getting this, the equivalent FIR filter must have linear-phase response. From (7), $H^M(z)$ and $H^M(z)^*$ are equal; therefore, in order to obtain a direct output with linear phase, $H^M(z)$ can be an odd or even order filter with symmetric coefficients (type I or II). On the other hand, $F^M(z)$ and $-F^M(z)^*$ are equal; therefore, in order to obtain a crossed output with linear phase, $F^M(z)$ must be an odd order filter with antisymmetric coefficients (type IV). It is a difficult task designing both $H^M(z)$ and its reciprocal $F^M(z)$ to be exactly linear-phase filters, but the effects of dispersion can be reduce by using low-order filters or by using an optimization process as the one proposed in Section 3.2. Even previous designs with dispersion of ± 50 ps/nm were claimed as linear-phase filters [23]. Anyway, in those cases where asymmetric interleaver is used to increase network traffic adding high bit rate channels at 40-Gb/s while keeping legacy 10-Gb/s systems, higher bit rate channels can be located in the null CD penalty output. This solution avoids using complex configurations as those reported in [9].

The proposed optimization process, based on GA, allows adjusting the interleaver response to desired values, as it is shown in Figs. 4 and 5 (first and second optimization examples, respectively). In the first optimization example, the pass bandwidths and isolation are highly improved, but the interleaver order and dispersion are increased to values below those reported in [10], for the same isolation. In the second optimization example, the pass bandwidth and isolation are also improved maintaining the interleaver order and slightly increasing its dispersion. The optimizations can be oriented to adjust specific parameters by using the appropriate objective function, as it is shown in Sections 3.1 and 3.2.

With the proposed optimization process, it is also possible to reduce the interleaver's order to $M = 4$ by removing the constraint that $H^M(z)$ has to be a filter with exactly linear-phase response.

In this case, the resulting maximum dispersion is ±50 ps/nm (±4 normalized), at both outputs, and the other parameters are maintained with good performance (isolation of -25 dB over 30% *FSR* and 13% *FSR* at *Tx* and *Ty*, respectively).

The dispersion of the interleaver outputs is defined by the linearity of the FIR filter that represents each output. It increases when increasing the output's box-like [4] characteristics.

Resulting dispersion of all examples are better than those obtained with MZRRI configuration in the order of ±200 ps/nm at 1550 nm without compensation [9] or equivalent to previous linear-phase designs in specific configurations [23].

GA can also be used for tolerance analysis and design optimization based on fabrication tolerances.

5. Conclusion

A general synthesis method for designing asymmetric flat-top birefringent interleavers has been reported. It uses a combination of digital signal processing approach and computational optimization by GAs. The method allows very good quality approximation of interleaver's specifications such as ripple, bands, and CD at both outputs. One output with linear phase can be achieved where higher bit rate channels can be allocated. A flat-top birefringent interleaver of seventh order with pass bandwidths of 43 GHz and 27 GHz, stop bandwidths of 11 GHz and 30 GHz, isolation of -25 dB over 11% FSR and 30% FSR, and CD of 0 ps/nm and ±63 ps/nm at the outputs *Tx* and *Ty*, respectively, has been designed. GA approach allows improving the stop bandwidth of *Tx* to 15 GHz and the isolation of *Tx* and *Ty* to -25 dB over 15% FSR and 30% FSR, respectively, maintaining the order and slightly increasing the CD. The interleaver isolation was also improved to -43 dB over 10% FSR and 22% FSR increasing the dispersion to ±85 ps/nm and the order to $M = 9$. Designs with dispersion bellow ±50 ps/nm at both outputs have also been reported. The priority between optimization parameters can be selected depending on the application.

Acknowledgment

References

[1] X. Yang and J. Zhang, "Optimum design of asymmetric birefringent interleaver based on FIR digital filter design technique," in *Proc. Microw. Conf., China-Jpn. Joint*, Sep. 10–12, 2008, pp. 595–598.

[2] H. Lu, K. Wu, Y. Wei, B. Zhang, and G. Luo, "Study of all-asymmetric interleaver based on two-stage cascaded Mach–Zehnder interferometer," *Opt. Commun.*, vol. 285, no. 6, pp. 1118–1122, Mar. 2012.

[3] S. Cao, J. Chen, J. N. Damask, C. R. Doerr, L. Guiziou, G. Harvey, Y. Hibino, H. Li, S. Suzuki, K. Y. Wu, and P. Xie, "Interleaver technology: Comparisons and applications requirements," *J. Lightw. Technol.*, vol. 22, no. 1, pp. 281–289, Jan. 2004.

[4] T. Chiba, "Waveguide interleaving filters," in *Proc. SPIE*, 2003, vol. 5246, pp. 532–538.

[5] B. B. Dingel, "Recent development of novel optical interleaver: Performance and potential," *Proc. SPIE*, vol. 5246, pp. 570–581, 2003.

[6] C. Lee, R. Wang, P. Yeh, and W. Cheng, "A new scheme of birefringent optical interleaver employing ring cavity as phase-dispersion element," presented at the Conf. Lasers Electro-Optics/Quantum Electron. Laser Science Conf. Photonic Applications Systems Technologies, OSA Tech. Dig. Series (CD) (Optical Society America), 2007, Paper JTuA30.

[7] S. A. Alboon and R. G. Lindquist, "Flat-top/distortionless tunable filters based on liquid crystal multi cavities for DWDM applications," in *Proc. IEEE Southeastcon*, 2008, pp. 117–122.

[8] W. Li, Q. Guo, and S. Gu, "Interleaver technology review," *Proc. SPIE*, vol. 4906, pp. 73–80, 2002.

[9] Y. Zhang, W. Huang, X. Wang, H. Xu, and Z. Cai, "High-extinction-ratio multipassband filter with flat-top and low-dispersion," *IEEE J. Quantum Electron.*, vol. 46, no. 6, pp. 860–870, Jun. 2010.

[10] R. H. Chu and G. Town, "Birefringent filter synthesis by use of a digital filter design algorithm," *Appl. Opt.*, vol. 41, no. 17, pp. 3412–3418, Jun. 2002.

[11] R. M. de Ridder and C. G. H. Roeloffzen, "Interleavers," in *Wavelength Filters for Fibre Optics*, H. Venghaus, Ed. Berlin, Germany: Springer-Verlag, 2006, pp. 381–432.

[12] Q. Wang and S. He, "Optimal design of a flat-top interleaver based on cascaded M-Z interferometers by using a genetic algorithm," *Opt. Commun.*, vol. 224, no. 4–6, pp. 229–236, Sep. 2003.

[13] B. Lyot, "Optical apparatus with wide field using interference of polarized light," *C.R. Acad. Sci. (Paris)*, vol. 197, p. 1593, 1933.

[14] Y. Ohman, "A new monochromator," *Nature*, vol. 141, no. 3563, pp. 157–291, Feb. 1938.

[15] K. Jinguji and M. Kawachi, "Synthesis of coherent two-port lattice-form optical delay-line circuit," *J. Lightw. Technol.*, vol. 13, no. 1, pp. 73–82, Jan. 1995.

[16] S. E. Vargas, "Contribución al diseño de filtros ópticos para redes con multiplexación en longitud de onda," Ph.D. dissertation, Escuela Politécnica Superior, Univ. Carlos III Madrid, Madrid, Spain, 2003, pp. 200-207.

[17] *Parks–McClellan Optimal FIR Filter Design,* MatWorks, Natick, MA, 2012. [Online]. Available: http://www.mathworks.es/help/toolbox/signal/ref/firpm.html

[18] *Asymmetric Optical Interleaver,* Optoplex Corp., Fremont, CA, 2011. [Online]. Available: http://www.optoplex.com/Asymmetric_Interleaver.htm

[19] C. K. Madsen and J. H. Zhao, *Optical Filter Design and Analysis: A Signal Processing Approach.* New York: Wiley, 1999.

[20] *Global Optimization Toolbox,* MatWorks, Natick, MA, 2012. [Online]. Available: http://www.mathworks.com/products/datasheets/pdf/global-optimization-toolbox.pdf

[21] L. Rosa, K. Saitoh, K. Kakihara, and M. Koshiba, "Genetic-algorithm assisted design of C-band CROW-miniaturized PCW interleaver," *J. Lightw. Technol.*, vol. 27, no. 14, pp. 2678–2687, Jul. 2009.

[22] O. S. Ahmed, M. A. Swillam, M. H. Bakr, and X. Li, "Efficient design optimization of ring resonator-based optical filters," *J. Lightw. Technol.*, vol. 29, no. 18, pp. 2812–2817, Sep. 2011.

[23] Q. J. Wang, Y. Zhang, and Y. C. Soh, "Design of linear-phase two-port optical interleavers using lattice architectures," *Opt. Lett.*, vol. 31, no. 16, pp. 2411–2413, Aug. 2006.